CORROSION SCIENCE AND TECHNOLOGY, Vol.18, No.6(2019), pp.258~266
[Research Paper]
pISSN: 1598-6462 / eISSN: 2288-65245
DOI: https://doi.org/10.14773/cst.2019.18.6.258

Study on Corrosion Properties of Additive Manufactured 316L Stainless Steel and Alloy 625 in Seawater

Geun-Su Jung[1], Yong-Ha Park[1], Dae-Jung Kim[2], and Chae-Seon Lim[1,†]

[1]*Materials and Coating Research, Samsung Heavy Industries, Geoje-si, Gyeongsangnam-do, 53261, Korea*
[2]*InssTek, Inc., 154 Sinseong-ro, Yuseong-gu, Daejeon, 34109, Korea*

(Received December 02, 2019; Revised December 17, 2019; Accepted December 17, 2019)

The objective of this study was to evaluate corrosion resistance of additive manufactured 316L stainless steel and alloy 625 powders widely used in corrosion resistance alloys of marine industry in comparison with cast alloys. Directed Energy Deposition (DED) method was used in this work for sample production. DED parameter adjustment was also studied for optimum manufacturing and for minimizing the influence of defects on corrosion property. Additive manufactured alloys showed lower corrosion resistance in seawater compared to cast alloys. The reason for the degradation of anti-corrosion property was speculated to be due to loss of microstructural integrity intrinsic to the additive manufacturing process. Application of heat treatment with various conditions after DED was attempted. The effect of heat treatments was analyzed with a microstructure study. It was found that 316L and alloy 625 produced by the DED process could recover their expected corrosion resistance when heat treated at 1200 °C.

Keywords: *Additive manufacturing, Corrosion, 3D printing, Nickel alloy, Directed energy deposition (DED)*

1. Introduction

Additive manufacturing (AM), also known as 3D printing, is relatively new technology as a manufacturing method for metallic materials compared to conventional manufacturing techniques such as casting and metal working. The products from AM are made stacking metallic materials in a layer by layer fashion according to CAD-drawn 3D models. The technique allows immense freedom in a dimension of the produced parts, enabling fabrication of complex-shaped parts that are very difficult or sometimes impossible to be realized otherwise. This is beneficial in multiple ways. A total weight of AM parts and manufacturing process time can be hugely saved. The part that is originally made by joining of smaller parts can be made in a single piece, improving productivity and also eliminating joint problems.

Due to the reasons described, additive manufacturing has been popular in many industrial and military fields of application for past decades [1,2,3]. However, it is not until recently that the technology starts to gain attention from the marine and shipbuilding industry. The effort to utilize the advantages of AM in the maritime sector has been made collaboratively by major shipyards and governmental bodies [4] for the special purpose parts. Classification societies are also making involvements in this current trend.

However, it is not completely certain whether the 3D printed metallic parts can meet high expectations of the shipbuilding industries. In most cases, metallic parts for marine purposes are a subject of many demands, e.g., structural load carrying capabilities, anti-corrosion properties and other functional purposes. In this work, 3D printed 316L stainless steel and alloy 625, actively used corrosion resistance alloys (CRA) in shipbuilding, are evaluated to study on their corrosion resistance in seawater, as seawater is a very important liquid actively utilized by the ship for ballasting, firefighting, and many other utility purposes. Due to the presence of chloride ions in seawater, the liquid tends to offer very harsh conditions to many metals.

2. Experimental Methods

The corrosion resistance of 3D printed 316L and alloy 625 are evaluated in comparison to the conventionally cast counterparts. Table 1 shows the chemistry of cast and 3D

†Corresponding author: chaeseon.lim@samsung.com

Table 1 Chemical composition of cast, 3D printed materials and metal power for 3D printing

Gr.	Type	C	Mn	Si	S	P	Cr	Ni	Mo	Fe	Nb	Co	Cu
316L	Cast	0.024	0.729	0.783	0.008	0.031	18.49	9.99	2.072	Bal.			
	3DP	0.01	1.052	0.5	0.01	0.007	18.29	11.51	2.358	Bal.			
	Powder	0.01	1.09	0.5	0.01	0.04	18.24	11.37	2.42	Bal.			
625	Cast	0.023	0.609	0.795	0.006	0.001	20.18	Bal.	8.86	2.75	3.14	0.018	0.02
	3DP	0.05	0.5	0.5	0.01	0.01	22.1	Bal.	9.25	3.59	3.58	0.18	0.07
	Powder	0.057	0.474	0.605	0.003	0.002	20.60	Bal.	9.42	3.65	3.40	0.213	0.016

printed materials along with the chemistry of the metal powder from which 3D printed products were made.

The used 3D printing method in this work is directed energy disposition (DED), which involves melting of metal powder, feed material, by the laser beam to build the desired shape. Commercially available metal powers were purchased and used as feed whose particle sizes are distributed within 45 ~ 150 microns in diameter for both stainless and nickel alloy cases. MK-1200 by InssTek Inc. capable of DED process was the used 3D printing machine for the current work. Fig. 1 shows the example of 3D printing work by DED.

In order to control a quality of the 3D printed material to maintain consistency throughout the research work, manufacturing parameters were optimized. The heat input controlled by laser power and the scan rate are the major parameters to control. Multiple lines with different manufacturing parameters were deposited on the same substrate to find the optimized parameters for 3D printing of 316L and alloy 625. The substrate material is 316L stainless steel.

Critical pitting temperature (CPT) and critical crevice temperature (CCT) are important references for seawater resistance of Ni-alloys. According to the ASTM standard for CPT and CCT testing [5], the cast and 3D printed sample with a size of 25 × 25 × 2 mm were ground using 120 grit sand papers, and pickled with acid solution (20% of HNO3 + 5% of HF + distilled water) for air passivation for 24 hrs before immersed in the bath filled with ferric chloride solution for 24 hrs. Temperature of the solution in the solution bath were controlled for the test. The samples were collected from the bath after each test session for visual inspection with weight measuring to define the CPT and CCT.

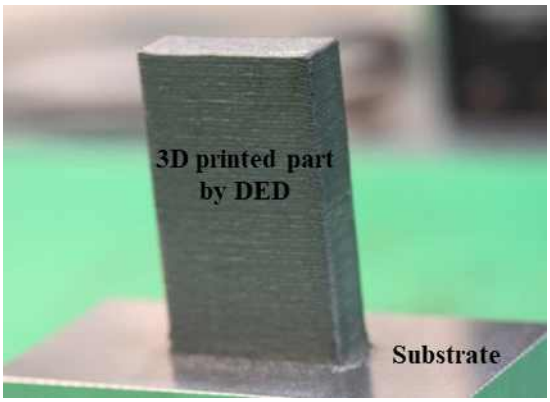

Fig. 1 3D printed sample by DED.

Additionally, 50 × 50 × 2 mm block samples were made for potentiodynamic polarization tests. Flat-cell type apparatus attached with potentionstats, Gamry Reference 3000, was used for the electrochemical experiments. Surfaces of the samples that are to the electrolyte were polished to the mirror surface using conventional preparation method. 3.5% NaCl solutions were used as electrolyte in the corrosion cell system. The scan range was from - 1.6 to 1.6 V with the scan rate of 1.6 mV/s. The flat surface of working/counter electrodes was exposed through 2.6 cm^2 hole to the electrolyte, and the reference (saturated calomel electrode, SCE) was placed near the working electrode for measurement. All electrochemical tests for the current work were conducted in ambient temperature.

It has been well established that metallic materials are typically heat-treated to control their properties after manufacturing. All cast samples for testing were provided after solution annealed for 3 hrs at 1065 and 1200 °C respectively for 316L and alloy 625. Heat treatment parameters for the cast samples were referenced for the 3D printed samples. Some of 3D printed samples were heat-treated for testing to see the effect of heat treatment on corrosion properties with heat treatment temperatures of 1065, 1130, and 1200 °C for both 316L and alloy 625. Water quenching was applied after 2 hrs of heat treatment in the electric furnace. The corrosion test results are discussed on the cast samples with heat treatment and the

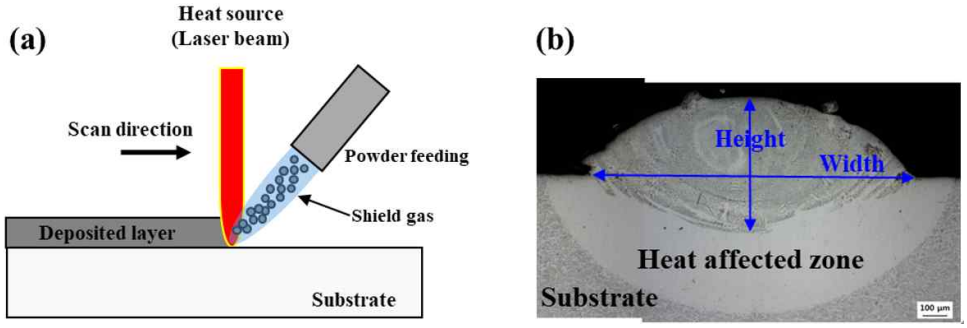

Fig. 2 Schematic of DED process (a), deposited layer by DED (b) [6].

3D printed samples with or without heat treatment based on their microstructures.

3. Results

3.1 3D printing process parameter optimization

In DED, a moving heat source will melt the feed metal in a powder form to create deposited layers on the metallic substrate to make a shape. This is schematically illustrated in Fig. 2a [6]. Fig. 2b shows the dimensions of the single-layer deposited on the substrate. Similar to the welded area, heat affected zone (HAZ) is observed buffering between the substrate and the deposited layer. It has been concluded that it is beneficial to maintain the height/width ratio close to 0.5. If the ratio is too low, the chemistry of the deposited layer may be altered by dilution with substrate, gradually affecting the material properties of the 3D printed part. If the ratio is close to 1, then it becomes difficult to create a layer with consistent shape. It is learnt from our experience that chemistry alteration by dilution and ill-balanced depositions are the causes of degradation in the material properties and defects such as porosity in the final product when multiple deposited layers are applied.

In order to optimize the process parameters for DED, lines with a single deposition for 316L and alloy 625 were made using various scan rates and laser powers on the substrate as shown in Fig. 3. The used scan rates are 0.7, 0.85 and 1.0 m/min, and the laser powers 500, 600, 700, and 800 W. Cuts were made perpendicular to the line direction to reveal the shape parameters of the depositions as shown in Fig. 4. Overall, it can be observed that, although productive, faster scan rates are not ideal for shape control. The best combinations of the parameters were determined for each alloy and summarized in Fig. 5. For 316L, 0.7 m/min of scan rate with 600 W of power is ideal for sample production, and for alloy 625, 0.7 m/min, and 800 W.

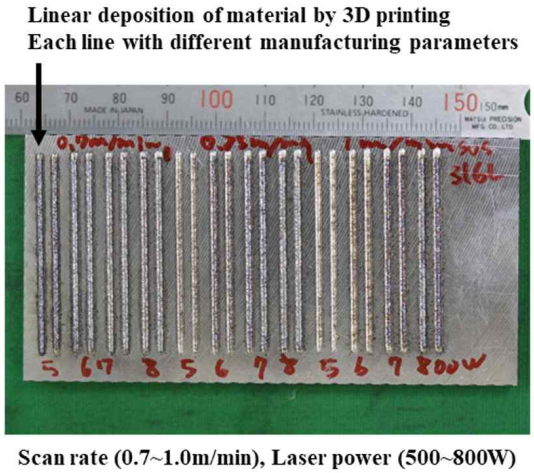

Fig. 3 Deposited lines with the different process conditions.

3.2 Evaluation of corrosion properties

Due to its abundance, seawater is fully utilized for the ocean going vessels. Unfortunately, seawater is a very corrosive liquid to stainless steels and Ni alloys because of chloride in seawater, which is known to break their passive films. Furthermore, it is also true that chloride attack becomes more active at the higher temperatures [6]. Chloride attack manifests itself as localized form of corrosion such as pitting and crevice corrosion, and the resistance to which are commonly expressed as CPT and CCT, resistance to pitting or crevice corrosion respectively. ASTM G48 suggests the testing method for determining CPT and CCTs. According to the ASTM standard, the starting temperature for the test can be estimated using the calculations below based on metal chemistry.

$$\text{CPT (°C)} = (2.5 \times \%\ \text{Cr}) + (7.6 \times \%\ \text{Mo}) + (31.9 \times \%\ \text{N}) - 41.0 \quad (1)$$

$$\text{CCT (°C)} = (1.5 \times \%\ \text{Cr}) + (1.9 \times \%\ \text{Mo}) + (4.9 \times \%\ \text{Nb}) + (8.6 \times \%\ \text{W}) - 36.2 \quad (2)$$

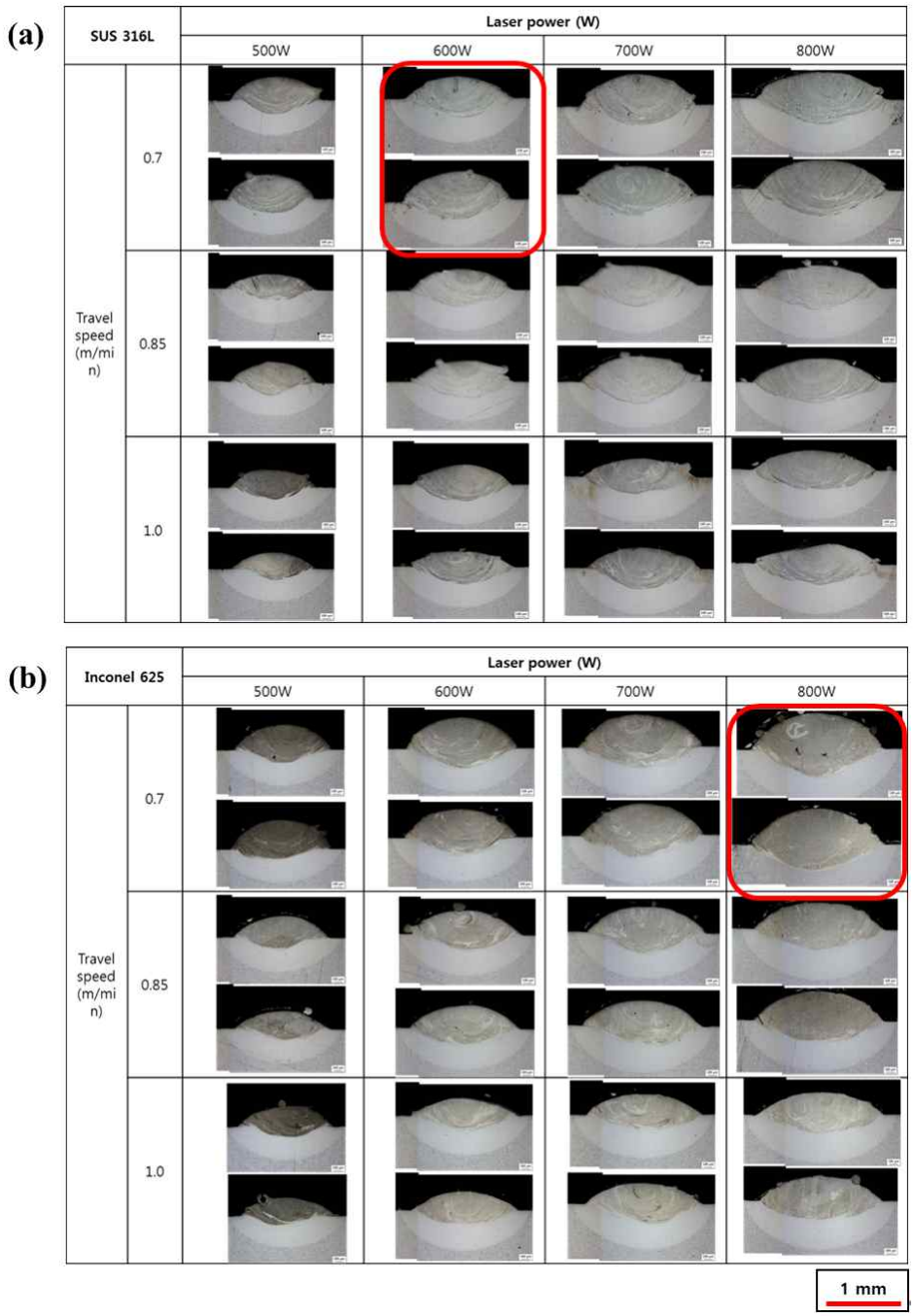

Fig. 4 Dimensions of the deposited layers with various conditions, (a) 316L, (b) alloy 625, optimized conditions are highlighted in red square.

$$CCT\ (°C) = (3.2 \times \%\ Cr) + (7.6 \times \%\ Mo) + (10.5 \times \%\ N) - 81.0 \quad (3)$$

Equation (2) is for the Ni base alloys, and (3) for the Fe base alloys. Above equations only give the quick reference as to alloy's resistance to localized Cl attacks. The calculated results are summarized in Table 2, whose values were used as a starting point for the following immersion test.

Table 3 and 4 show the immersion test results for 316L and alloy 625 respectively, where X means pitting or crevice corrosion took place after the test. It is noticed that cast 316L has better pitting resistance than 3D printed counterparts. On the contrary, overall localized corrosion

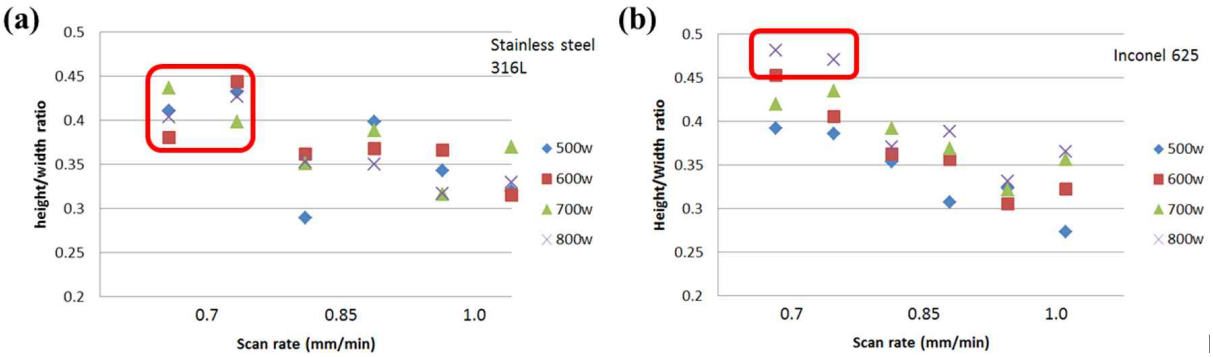

Fig. 5 Height/width ratio of the depositions with various conditions, (a) 316L, (b) alloy 625.

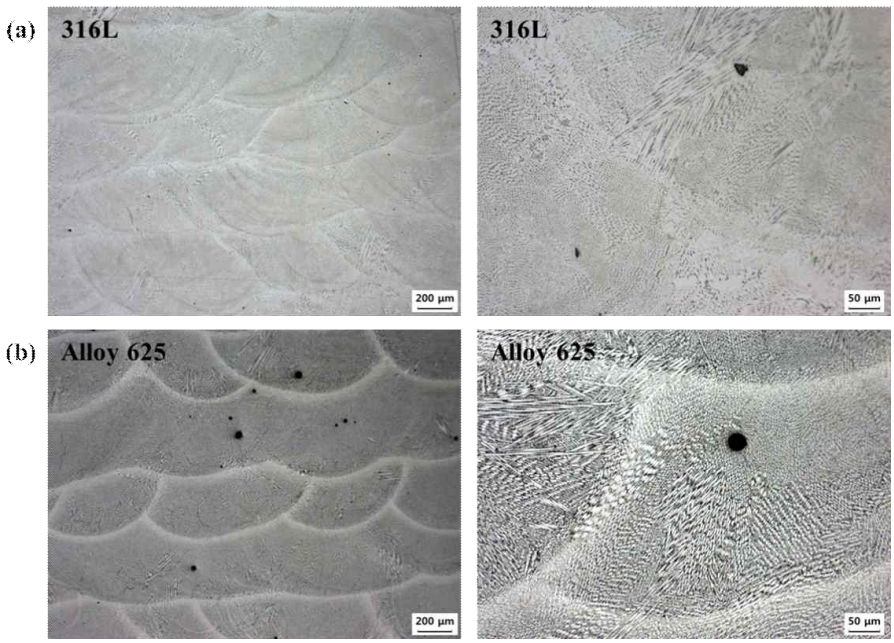

Fig. 6 Microstructure of 3D printed materials, (a) 316L, (b) alloy 625, showing micro-defects in microstructure.

resistance is much better for 3D printed alloy 625. The reason for the inferior CPT of 3D printed 316L may be explained with its microstructure as shown in Fig. 6, where many porosities or defects can be found. However, 3D printed alloy 625 despite bearing similar defects within its microstructure do not show lower corrosion resistance than the cast sample, implying that there can be other factors for corrosion properties of the alloy.

Fig. 7 and 8 are corrosion rate of the alloys at each immersion condition. The corrosion rate is expressed in MPY (mils per year). In the case of 316L, overall mass

Table 2 Calculated CPT and CCT for Cast and 3D printed materials

	Type	CPT (°C)	CCT (°C)
316	Cast	21	-6
	3DP	23	-5
	Powder	23	-4
625	Cast	78	26
	3DP	85	32
	Powder	82	29

Table 3 CPT and CCT determined by immersion test for 316L (O: no corrosion, X:pitting or crevice corrosion)

Test	Type	Temperature (°C)		
		15	10	5
CPT	3DP	X	X	X
	Cast	X	O	
CCT	3DP		X	X
	Cast		X	X

Table 4 CPT and CCT determined by immersion test for alloy 625 (O: no corrosion, X:pitting or crevice corrosion)

Test	Type	Temperature (°C)							
		70	60	55	50	45	40	35	30
CPT	3DP	X	X	X	O				
	Cast	X	X	X	X	X	O		
CCT	3DP					X	O		
	Cast							X	O

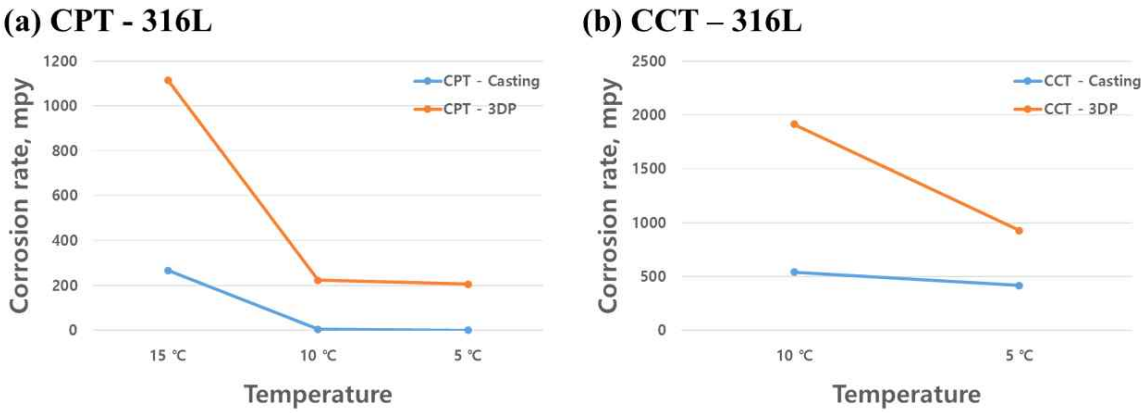

Fig. 7 CPT, CCT determination by corrosion rate for 316L.

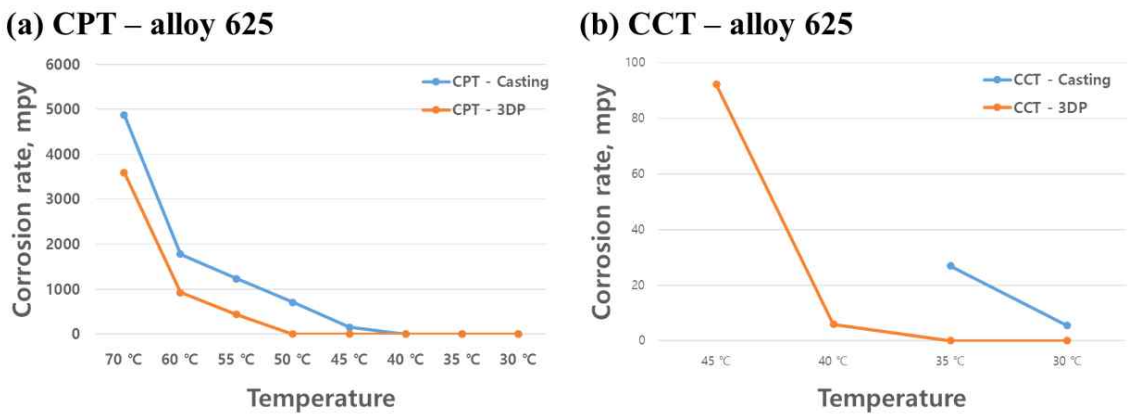

Fig. 8 CPT, CCT determination by corrosion rate for alloy 625.

loss is much higher for the 3D printed samples, whereas the opposite is true for alloy 625.

It was recognized that heat treatment may be necessary to optimize the corrosion properties of the 3D printed alloys. Table 5 and 6 compare the immersion test results of the 3D printed samples with heat treatment and the ones without. The improvement in the resistance to localized corrosion can be readily observed for both cases.

Fig. 9 shows the results of potentiodynamic polarization experiments. The result shows that the passive films formed on 3D printed samples broke down earlier than the cast samples. It is speculated that the 3D printing needs to be followed by an additional process that ensure the microstructure control. Fig. 10 compares the polarization curves of heat treated 3D printed samples to the cast sample. The gradual increase in corrosion property is noticed with the increasing heat treatment temperature. From the experimented curves, corrosion parameters of importance are summarized as shown in Table 7, which are the corrosion potential (E_{corr}), pitting potential (E_{pit}), and ΔE, the difference between E_{corr} and E_{pit}. ΔE is the representative of the passive region of the material. The larger

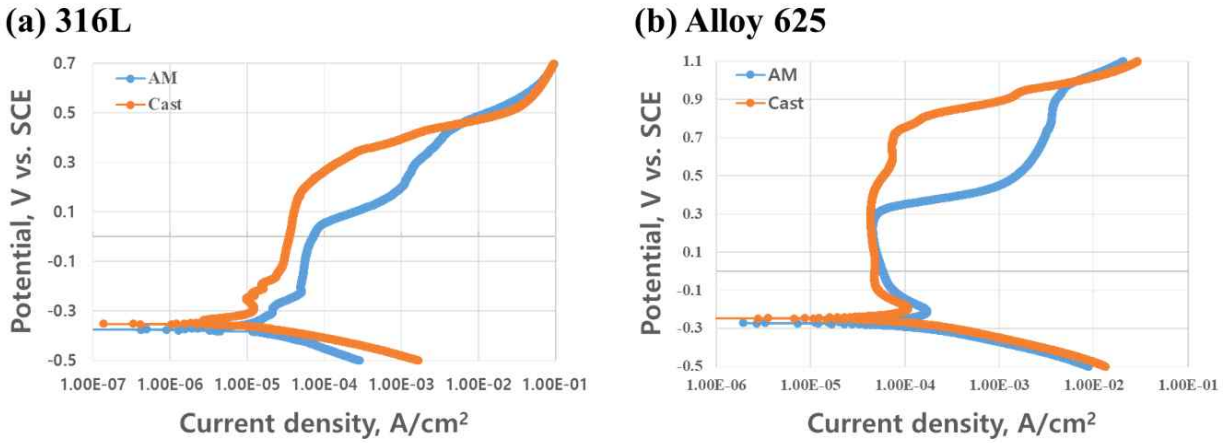

Fig. 9 Polarization curves for the 3D printed and cast alloys, (a) for 316L, (b) for alloy 625.

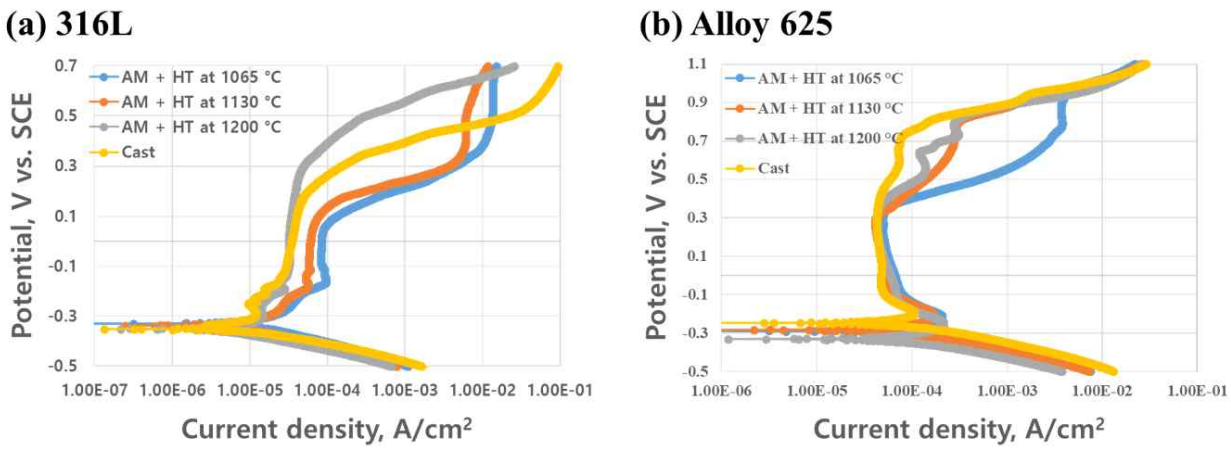

Fig. 10 Polarization curves for the effect of heat treatment, (a) for 316L, (b) for alloy 625.

Table 5 CPT and CCT comparison for 3D printed 316L, effect of heat treatment (O: no corrosion, X:pitting or crevice corrosion)

Test	Type	Temperature (°C)		
		15	10	5
CPT	3DP	X	X	X
	1065 °C		O	O
	1130 °C		X	O
	1200 °C		O	O
CCT	3DP		X	X
	1065 °C		X	X
	1130 °C		X	X
	1200 °C		X	X

Table 6 CPT and CCT comparison for 3D printed alloy 625, effect of heat treatment (O: no corrosion, X:pitting or crevice corrosion)

Test	Type	Temperature (°C)							
		70	60	55	50	45	40	35	30
CPT	3DP	X	X	X	O				
	1065 °C			X	O				
	1130 °C		X	O					
	1200 °C		X	O					
CCT	3DP					X	O		
	1065 °C					X	O		
	1130 °C					X	O		
	1200 °C						X	O	

Table 7 Corrosion parameters from the polarization curves

	Type	Ecorr, V	Epit, V	ΔE = Epit-Ecorr, V
316L	3DP	- 0.375	0.036	0.411
	1065 ℃	- 0.33	0.048	0.378
	1130 ℃	- 0.338	0.094	0.432
	1200 ℃	- 0.35	0.251	0.601
	Cast	- 0.352	0.178	0.53
625	3DP	- 0.248	0.306	0.554
	1065 ℃	- 0.285	0.333	0.618
	1130 ℃	- 0.284	0.287	0.571
	1200 ℃	- 0.331	0.368	0.699
	Cast	- 0.247	0.438	0.685

the value, the more stable the passive film, and hence the more resistant material to chloride attack. According to the test results, ΔE is the largest when the both samples were heat treated at 1,200 °C.

Combining CPT and CCT test results and the polarization results, 1,200 °C seems to be the ideal heat treatment temperature for 316L and alloy 625, yielding the best corrosion properties overall. It is confirmed that by optimization of the heat treatment, 3D printed materials can be as corrosion resistant as conventionally produced materials such as castings.

The microstructures of the 3D printed samples were studied as shown in Fig. 11. The sign of the scanning pattern from the deposition process remains in the as 3D printed microstructure, which could have influenced corrosion properties of the material. It is evident that the samples underwent the recrystallization in the furnace during the heat treatment, as more homogeneous microstructure can be seen from the heat-treated samples. This can be attributed to the improved corrosion properties of the 3D printed samples after heat treatment.

4. Conclusion

The corrosion properties of the two commonly used corrosion resistance alloys, 316L stainless steel and alloy 625, are studied, and the following conclusions are summarized below.

1) The deposition parameters for 3D printing of the currently investigated alloys have been optimized to avoid chemical dilution with substrate and maintain the deposited layer consistent in shape. The scan rate of 0.7 m/min is accepted for both 316L and alloy 625, while the laser power of 600 W is ideal for 316L and 800 W for alloy 625.
2) Corrosion properties of the 3D printed alloys are generally inferior to the casting alloys, and this is due to the microstructure. Microstructure needs to be controlled via heat treatment for the investigated alloys to have their expected corrosion properties.
3) Beneficial effect of the heat treatment on corrosion properties of the 3D printed materials has been confirmed via experiments. Increase in the pitting potential and the enlargement of the passive region were observed from the electrochemical tests with heat-treated samples.

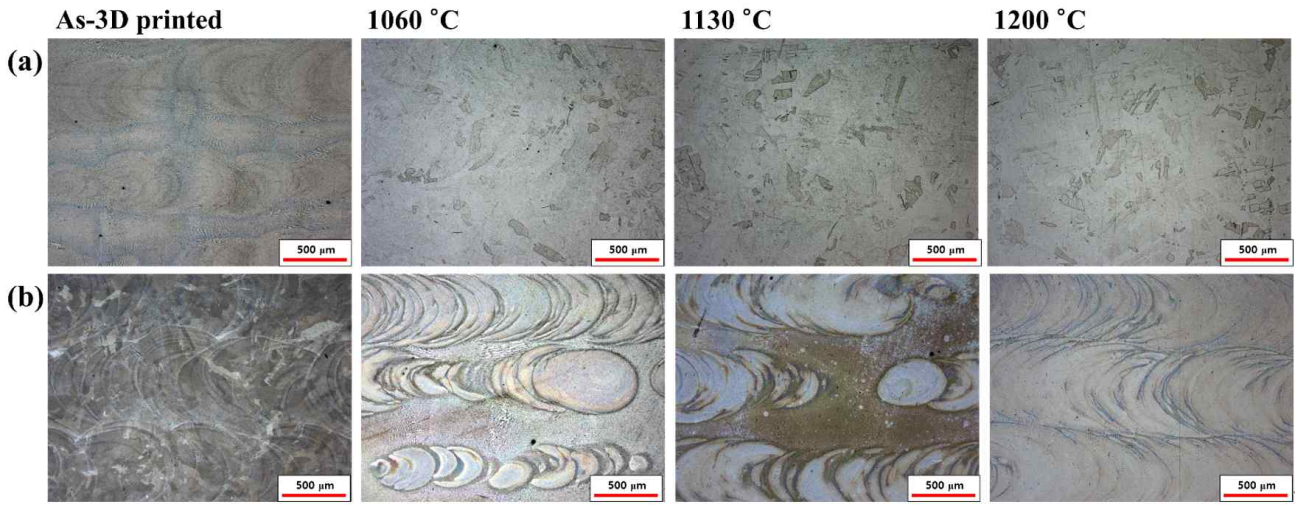

Fig. 11 The effect of heat treatment on microstructure evolution of 3D printed alloys, (a) for 316L, (b) for alloy 625.

4) Suggested heat treatment temperature for the 3D printed 316L and alloy 625 is 1,200 ℃. The samples heat treated at such temperature gave the optimum corrosion properties.

According to the experiment findings, it is reasonable to suspect that mechanical properties for the 3D printed materials can also be improved through correct microstructure control. In this work, the conventional furnace heating was used for heat treatment. It may be considered as a future work that use of heat source that is used for melting of the feed metal and depositing it can be used as a burner for local heat treatment of the 3D printed product on spot.

Acknowledgments

This study was supported by the R&D project of Ministry of Trade, Industry and Energy (MOTIE) titled as 'Dissimilar metal valve development based on 3D printing technology with 20 % increased corrosion and wear resistant' (Code No. 200004739), Republic of Korea.

References

1. D. Herzong, V. Seyda, E. Wycisk, and C. Emmelmannm, *Acta Mater.*, **117**, 15 (2016).
2. B. A. Szost, S. Terzi, F. Martina, D. Boisselier, A. Prytuliak, T. Pirling, M. Hofmann, and D. J. Jarvis, *Mater. Design*, **89**, 5 (2016).
3. S. Das, D. Bourell, and S. Babu, *MRS Bull.*, **41**, 10 (2016).
4. I. Moltk, Maritime guide to 3D print, http://greenship.org (2016).
5. ASTM G48, Standard test methods for pitting and crevice corrosion resistance of stainless steels and related alloys by use of ferric chloride solution (2015).
6. J. C. Benedyk, *Additive manufacturing of aluminum alloys*, http://www. Lightmetalage.com (2018).
7. A. J. Sedriks, *Corrosion of Stainless Steels, 2nd ed.*, p. 208, John Wiley & Sons, New York (1996).